







# HYBRID RECONFIGURABLE INTELLIGENT METASURFACES

## *Enabling Simultaneous Tunable Reflections and Sensing for 6G Wireless Communications*

George C. Alexandropoulos , Nir Shlezinger , Idban Alamzadeh ,  
Mohammadreza F. Imani , Haiyang Zhang , and Yonina C. Eldar 

XXXXX

**T**he latest discussions on upcoming 6G wireless communications are envisioning future networks as a unified communications, sensing, and computing platform. The recently conceived concept of the smart radio environment, enabled by reconfigurable intelligent surfaces (RISs), contributes toward this vision, offering programmable propagation of information-bearing signals. Typical RIS implementations include metasurfaces with almost passive unit elements capable of reflecting their incident waves in controllable ways. However, this solely reflective operation induces significant challenges for RIS optimization from the wireless network orchestrator. For example, RISs lack information to locally tune their reflection pattern, which can be acquired only by other network entities and then shared with the RIS controller. Furthermore, channel estimation, which is essential for coherent RIS-empowered communications, is challenging with the available RIS designs. This article reviews the emerging concept of hybrid reflecting and sensing RISs (HRISs), which enables metasurfaces to reflect the impinging signal in a controllable manner while

simultaneously sensing a portion of it. The sensing capability of HRISs facilitates various network management functionalities, including channel parameter estimation and localization, while giving rise to potentially computationally autonomous and self-configuring metasurfaces. We discuss a hardware design for HRISs and detail a full-wave electromagnetic (EM) proof of concept. The distinctive properties of HRISs, in comparison to their solely reflective counterparts, are highlighted, and a simulation study evaluating HRISs' capability for performing full and parametric channel estimation is presented. Future research challenges and opportunities arising from the HRIS concept are also included.

### Introduction

The potential of RISs for programmable EM wave propagation has recently motivated extensive interest as a candidate smart connectivity paradigm for 6G wireless networks [1], [2]. RIS technology, which typically refers to artificial planar structures with almost passive electronics, is envisioned to be jointly optimized with conventional transceivers [3] to significantly boost wireless systems in terms of coverage and energy efficiency while satisfying regulated EM field emissions.

Digital Object Identifier 10.1109/MVT.2023.3332580

Date of current version: 11 December 2023

The typical RIS unit element is the meta-atom, which is usually fabricated to realize multiple programmable states corresponding to distinct EM responses. By externally controlling these states, various reflection and scattering profiles can be emulated [4]. The RIS implementations to date do not include any power amplification circuitry; hence, they consist of metasurfaces acting only as tunable reflectors. While passive RISs enable programmable wireless environments, their solely reflective operation induces notable challenges. For instance, the fact that conventional RISs cannot sense the environment implies that they lack information to dynamically configure their reflection pattern. For this reason, they are typically externally configured by a dedicated network entity, or a base station (BS), via dedicated control links, which in turn complicates their deployment and management [5]. Furthermore, the inclusion of an RIS implies that a signal transmitted from a user terminal (UT) to a BS encounters at least two channels: the UT-RIS and RIS-BS channels. Estimating these individual channels is a challenging task due to the reflective nature of RISs [4], which significantly limits the ability to reliably communicate in a coherent manner. In addition, solely reflective RISs impose challenges on wireless localization [6]. To overcome the obstacles, it was recently proposed to equip RISs with a dedicated external device consisting of a few reception radio-frequency (RF) chains [7], enabling low-cost signal reception and processing.

Radiating metasurfaces have recently emerged as a promising technology for realizing low-cost and low-power extremely large multiple-input, multiple-output (MIMO) antenna arrays [8]. Dynamic metasurface antennas (DMAs) pack large numbers of controllable radiative meta-atoms that are coupled to one or several waveguides, resulting in MIMO transceivers with advanced analog processing capabilities. While the implementation of DMAs differs from reflective RISs, the similarity in their meta-atom structure indicates the feasibility of designing hybrid reflecting and sensing elements. Metasurfaces consisting of such meta-atoms can reflect their impinging signals while simultaneously measuring portions of them [9]. Such HRISs bear the potential of significantly facilitating RIS orchestration without notably affecting the coverage extension advantages offered by conventional RISs.

In this article, we review the emerging concept of HRISs and discuss their possible prominent applications for future wireless communications. We first review the possible configurations for hybrid meta-atoms and showcase the feasibility of HRISs by describing an implementation of simultaneously reflecting and sensing meta-atoms, based on [9], accompanied with full-wave EM simulations. We proceed with the investigation of the potential of HRISs for wireless communications, demonstrating their ability to achieve desired reflection

patterns while using their sensing capability to locally estimate angles of arrival (AOAs), enabling their sensing autonomy and, consequently, self-configuration. Then, we highlight their distinctive properties in contrast to solely reflective RISs and active relays. In particular, we show that, as opposed to active relays, HRISs preserve the power-efficient reflective operation of conventional RISs, as they do not require any transmission circuitry and can perform sensing with a very small number of reception RF chains. Compared to equipping conventional RISs with dedicated receivers [7], HRISs allow sensing the signals observed at each hybrid reflecting and sensing element and implement reception at their side. A simple model for HRIS dual operation is introduced, facilitating a representative simulation study of the HRIS capability for signal parameter sensing and channel estimation. We conclude with a description of research challenges and opportunities with HRISs, including key experimental directions that are expected to further unveil the potential role of HRISs in 6G wireless networks.

### HRIS Design and Proof of Concept

In all available fabricated designs [4], RISs are incapable of any sort of sensing of the impinging signal. The concept of RISs realizing sensing and communicating was first envisioned in [9], where an implementation with sensing capabilities at the meta-atom level was demonstrated. We next present HRISs incorporating this hybrid meta-atom design and that leverage previous works on DMAs [8] to integrate sensing into each meta-atom without losing their reconfigurable reflection functionalities.

### Configurations of Hybrid Meta-Atoms

From a hardware perspective, two different configurations, allowing for meta-atoms to both reflect and sense, can be designed. The first consists of hybrid meta-atoms, which simultaneously reflect a portion of the impinging signal while enabling another portion to be sensed [9]. The second configuration uses meta-atoms that reconfigure between near-perfect absorption and reflection. In the latter case, each meta-atom has two modalities [10]: it can either sense the received signal (absorption mode) or, once necessary information is extracted, reflect the signal toward a desired direction (reflection). While the configurations vary in their implementation, in terms of modeling, the first configuration may be viewed as a generalization of the second since a hybrid meta-atom can be tuned to fully absorb or sense. Accordingly, we focus henceforth on the first case, relying on hybrid meta-atoms, as illustrated in Figure 1. Such HRISs are realized by adding a waveguide to couple to each or groups of meta-atoms. Each waveguide can be connected to a reception RF chain, allowing the HRIS to locally process a portion of the received signals in the digital domain.

However, the elements' coupling to waveguides implies that the incident wave is not perfectly reflected. In fact, the ratio of the reflected energy to the sensed energy is determined by the coupling level. By keeping this waveguide near the cutoff, we can reduce its footprint while also reducing coupling to the sampling waveguide.

### Design Considerations

An important consideration in HRIS design is the interelement spacing. To accurately detect the phase front of the incident wave, the spacing of adjacent meta-atoms needs to be smaller than half a wavelength. However, this imposes constraints on the meta-atom size, which is accommodated via the multilayer structure in Figure 1. Another important factor to consider is the necessary circuitry to detect the signal coupled from each meta-atom; in particular, each waveguide should be connected to an RF chain. Since the incident wave on the HRIS may couple to all sampling waveguides (with different amplitudes), we can think of the combination of the metasurface and the sampling waveguides as a receiver structure with equivalent analog combining.

The sensing circuitry, however, adds another factor to consider when designing an HRIS: while closer element spacing improves the ability to direct the reflected signal to a desired direction (with smaller side-lobes) and increases the accuracy of detecting incident wavefronts, close element spacing increases the total number of meta-atoms and, consequently, the cost and, potentially, the power consumption. Nonetheless, this can be balanced by limiting the number of RF chains—which are connected to the waveguides and not directly to each meta-atom—and profiting from each meta-atom's controllable analog processing nature. The latter feature also contributes to reducing the cost and power consumption of the introduced sensing circuitry, which

does not appear in conventional RISs that are incapable of sensing.

### Implementation

Most RIS elements in available designs are resonators, which can be easily modified to couple to a waveguide. For example, the meta-atom in [11] requires a via to deliver the dc signal to this element in order to tune the switchable component. To eliminate the undesired coupling from the RF signal to the dc bias line, this via is usually terminated in a radial stub. In the hybrid meta-atom implementation proposed in [9], we utilized this coupling to implement sensing of the incident signal. One can envision a design where the via is attached to two copper traces, one to sample the signal and the other to transfer the dc signal (which is connected to a radial stub), though confining the coupled RF signal to such a copper trace may be challenging. A substrate-integrated waveguide (SIW), which is effectively a rectangular waveguide, is used to capture the sampled wave, as shown in Figure 1. By changing the annular ring around the coupling via or the geometrical size of the SIW, the HRIS can realize different coupling strengths.

### Full-Wave EM Simulations

The hybrid meta-atom illustrated in Figure 1 is loaded by a varactor, whose effective capacitance is changed by an external dc signal, consequently changing the reflection phase of its impinging wave. By properly designing the phase variation along the HRIS, the reflected wave can be steered toward desired directions. To evaluate the ability of our HRIS design to simultaneously reflect while sensing its incident signal, we next present a full-wave simulation study using Ansys HFSS. We first evaluate a hybrid meta-atom operating at 19 GHz, focusing on its reflection and coupled components in Figure 2. It is demonstrated that this element can be tuned to reflect and sense different portions of its impinging signal [Figure 2(a)] while applying controllable phase shifting to the reflected signal [Figure 2(b)]. Additional investigations of a full HRIS consisting of such hybrid meta-atoms, further showcasing the design's validity, are available in [9].

### HRISs for Smart Wireless Environments

In this section, we discuss how the concept of HRISs, via the previously described implementation guidelines, can be exploited to facilitate

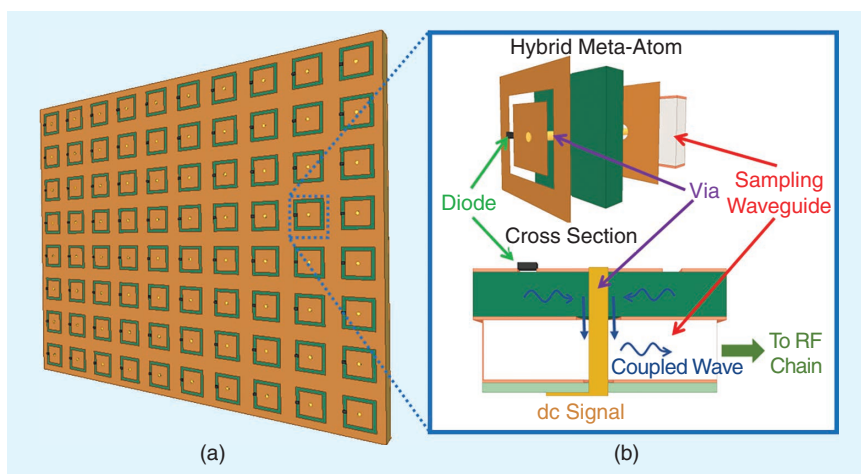


**FIGURE 1** The (a) designed HRIS and the (b) constitutive hybrid meta-atom design proposed in [9]. In (b), the layers of the meta-atom are artificially separated for visualization purposes, and the cross section of the metasurface as well as the coupled wave signal path are depicted.

wireless operations. We first describe the envisioned HRIS-empowered wireless communications paradigm and then present a simple model encapsulating the simultaneous tunable reflection and sensing operations of HRISs. Finally, some numerical results corroborating the potential of HRISs for AOA recovery and full channel estimation are presented.

### HRIS-Empowered Wireless Communications

The most common application of conventional RISs is to facilitate communications between UTs and a BS [2] by shaping information-bearing signals over the air to overcome harsh nonline-of-sight conditions and improve coverage. In such setups, the RIS tunes its meta-atoms to generate favorable signal propagation profiles. To achieve this, the BS maintains a control link with the digital controller of the RIS, where the latter sets the configuration of each meta-atom according to the control messages received by the BS. This setup can be also extended to multiple RISs and cloud-controlled networks [5]. This form of RIS-aided communications gives rise to several challenges. For instance, the fact that the RIS must be remotely controlled by the BS complicates the RIS's deployment and network management. Moreover, in the absence of direct channels between the BS and UTs, the former observes only the transmitted signals that propagated via the

RIS-parameterized channel, namely, the composition of the UTs–RIS channel, the RIS reflection configuration, and the RIS–BS channel. The fact that one cannot disentangle this combined channel implies that the BS cannot estimate its individual components but only the composite form [12]. This property not only reflects on the ability to estimate the channels but also limits the utilization of some network management tasks, such as wireless localization and sensing.

We envision HRISs to be utilized at least for the same purposes as conventional solely reflective RISs. This includes, for instance, the typical application of coverage extension and connectivity boosting by modifying the propagation profile of information-bearing EM waves, as demonstrated in Figure 3. Similar to setups involving a conventional RIS [2], the BS can maintain a dedicated control link with the HRIS, though the latter can also operate independently due to its sensing capability. For instance, the HRIS can use its collected estimations for the AOA of intended impinging signals to decide its phase configuration, thus relieving its dependence on external configuration and control [13]. Nonetheless, when such a control link is present, it should not be used solely for unidirectional control messages from the BS to the metasurface, as in reflective RISs, but now the HRIS can also use it to convey some sensed information to the BS. The fact that the UTs' transmissions are also captured

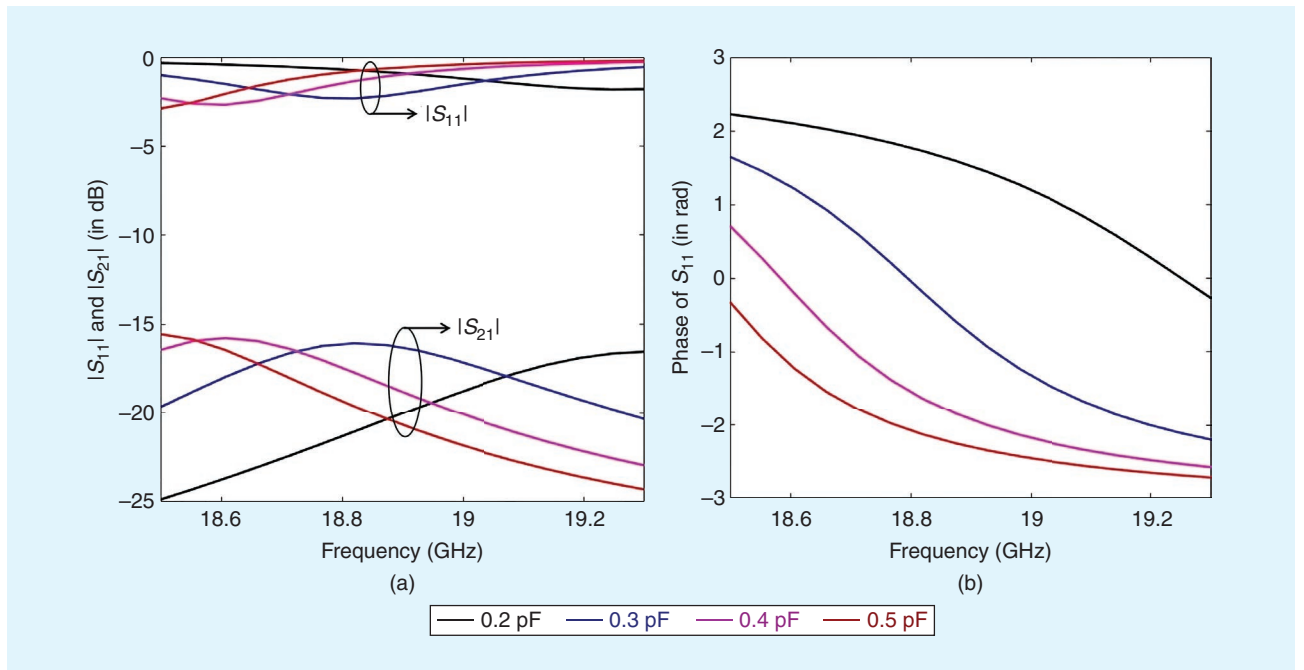


**FIGURE 2** A full-wave EM simulation of a single hybrid meta-atom [9] around the operating frequency 19 GHz. (a) The  $S_{11}$  parameter indicates the reflection from the meta-atom, while the  $S_{21}$  parameter represents the coupling to its sampling waveguide. The dip in the magnitude of  $S_{11}$  indicates the resonance of this element that changes as a function of the effective capacitance of the deployed varactor diode. The magnitude of the coupling  $S_{21}$  to the sensing waveguides has been kept below  $-15$  dB to ensure that ample power is reflected by this meta-atom. It is depicted that the coupling changes as a function of the effective capacitance of the varactor diode. (b) The corresponding reflection phase of the hybrid meta-atom changes as a function of the effective capacitance of the varactor diode. This change in phase can be used to generate different reflection patterns, enabling the redirection of the impinging signal on the meta-atom toward different directions.

by the HRIS can notably improve channel estimation, as discussed in the following, which in turn facilitates coherent communications. Furthermore, the sensed signal can be used for localization, RF sensing, and radio mapping [6].

As opposed to using reflective RISs that incorporate a few dedicated receive elements [7] within their structure for channel estimation, HRISs profit from their entire panel to sense part of their impinging signals during periodic acquisition phases, while being capable to operate in fully reflective mode during data transmission. They can be also deployed for simultaneous channel estimation and data communication via blind estimation techniques. It is noted that the concept of receiving (semi-passive) RISs [4] can be implemented with a special case HRIS having all its meta-atoms configured to fully sense. An additional key difference between wireless networks empowered by HRISs and solely reflective RISs stems from the fact that the former do not reflect all the energy of the incident signal (when the HRIS is also configured to sense) since a portion of it is sensed and collected by the HRIS local processor. Nevertheless, this may degrade the signal-to-noise ratio (SNR) at the BS.

The potential benefits of HRISs over solely reflective RISs come with additional energy consumption and cost. While the proposed meta-atom design in Figure 1 is passive, as are solely reflective RISs, HRISs require

additional power for locally processing the sensed signals. The utilization of RF chains and the additional analog combining circuitry, which are not required by conventional RISs, is translated into increased cost. While explicitly quantifying this increased cost and power consumption is highly subject to the specific implementation, it is emphasized that an HRIS is still an RIS and not an active multiantenna relay. Namely, it does not involve a power-consuming wireless transmission mechanism for amplifying and transmitting its received signals and is thus expected to maintain the cost and power gains of metasurfaces over traditional relays [2]. An additional challenge associated with HRISs stems from the optional need for a bidirectional control link between an HRIS and the BS. This link can be used for making the HRIS's observations available to the BS (otherwise, they remain local) to support higher throughput compared to the unidirectional control link utilized by conventional RISs.

### Model for Simultaneous Reflection and Sensing

A simple, yet generic, model for HRIS operation can be obtained by considering the HRIS's reflective and sensing capabilities individually. As discussed in the "HRIS Design and Proof of Concept" section, the HRIS tunable reflection profile is similar to conventional RISs, where it is typically modeled as controllable phase shifters.

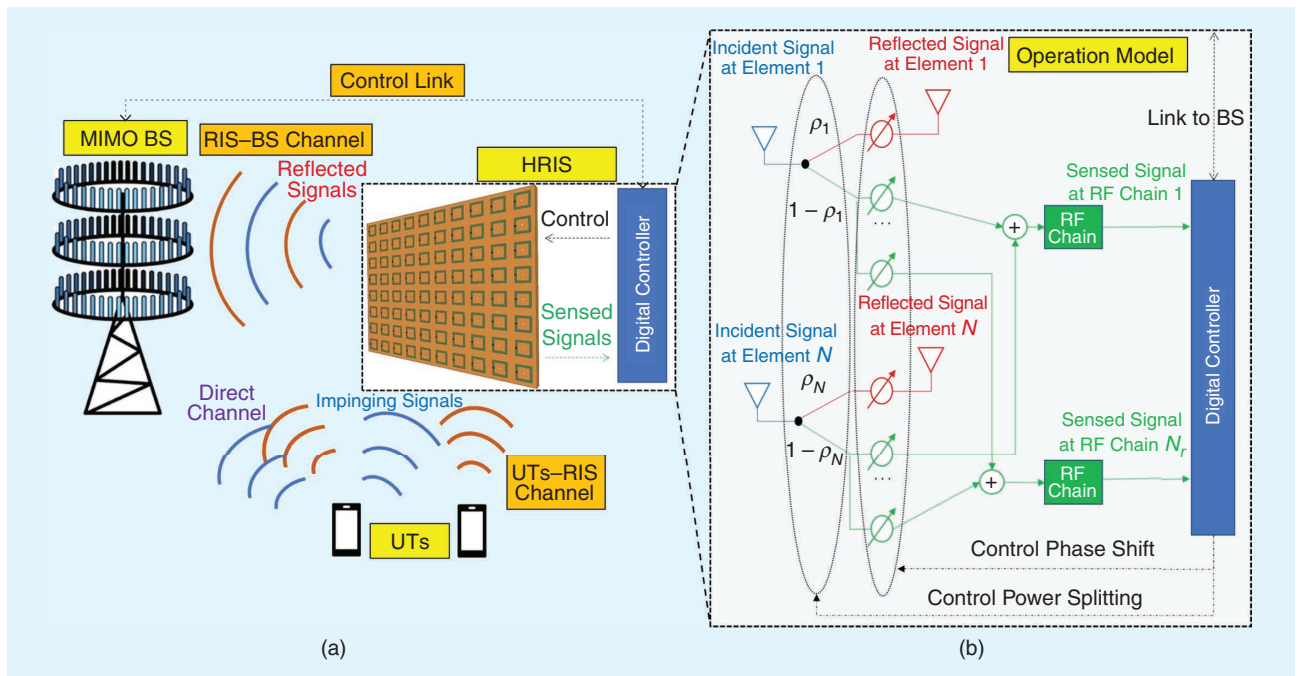


**FIGURE 3** The (a) uplink of multiuser MIMO systems incorporating the proposed HRIS structure that also senses a portion of the impinging UT signals and the (b) operation model of the HRIS. In this model, the HRIS consists of  $N$  hybrid meta-atoms. The incident signal at each meta-atom is split into a portion that is reflected (after tunable phase shifting) in the environment, while the remainder of the signal is sensed and processed locally at the metasurface. Parameter  $\rho_n$  ( $n = 1, 2, \dots, N$ ) represents the coupling coefficient (i.e., the power splitting ratio between reflection and sensing operations) for each  $n$ th meta-atom. The received portion of the impinging signal undergoes each element's controllable sensing response and is collected at the  $N_r$  reception RF chains connected to the  $N$  sampling waveguides ( $N \gg N_r$ ). The digital outputs of these RF chains are processed by a digital processor.

However, unlike conventional RISs, in HRISs, the reflectivity amplitude for each meta-atom is determined by a design knob that can be adjusted by changing the amount of coupling to the sensing circuitry. This design knob is modeled by a parameter  $\rho_n \in [0, 1]$  representing the portion of the signal energy being reflected by each  $n$ th hybrid meta-atom. This parameter is related to the amount of coupling between the meta-atom and the sampling waveguide, which essentially determines how much loss the HRIS introduces compared to solely reflective RISs. Note that if the coupling is too small, the sensed signal at the HRIS becomes susceptible to noise, while when it is too high, the signal reflected is considerably attenuated. As a result, it is useful to consider the reflectivity amplitude a design knob and optimize its acceptable range given a desired wireless system operation.

The second part of the HRIS model describes the relationship between the impinging waveform at the HRIS and the field values picked up by the HRIS sensing circuitry. The exact details of this model are heavily dependent on the specific implementation (see the “Research Challenges and Opportunities” section for more details). For simplicity, one can consider this relationship to be as simple as the nonreflected part (i.e.,  $1 - \rho_n$ ) multiplied by a phase component. Finally, as in DMAs [8], the RF chains via which the sensed signals are forwarded to the digital processor are connected to the waveguides, and thus, the sensed signal path can be viewed as a hybrid analog and digital receiver.

The resulting HRIS operation model is illustrated in Figure 3(b), where one can configure the portion of the reflected energy for each meta-atom as well as the phase shifting carried out at the reflected and received signal paths. We note that the HRIS may be configured to realize solely reflective RISs [2] (by setting  $\rho_n = 1$  for each  $n$ th element) or the partially receiving RISs in [7] (by setting  $\rho_n = 0$  for some  $n$  values and  $\rho_n = 1$  for the remaining  $n'$  values) or semi-passive RISs [4] (by setting  $\rho_n = 0$  for each  $n$ th element). Accordingly, any performance achievable with the latter RISs is also achievable with an HRIS. However, HRISs provide increased flexibility, as the operation of their meta-atoms can be configured based on any current conditions, which greatly facilitates HRIS self-automation and adaptivity [14]. In practice, the parameters of the

hybrid meta-atoms are typically coupled, implying that one cannot tune them arbitrarily. However, this relatively simple model provides an understanding of what one can gain by properly tuning these HRIS parameters, as detailed in the following section.

### Channel Estimation With HRISs

We next investigate the contribution of the sensing capability of HRISs in two indicative applications: 1) estimation of the AOA of an impinging signal and 2) estimation of the end-to-end channel matrices in multiuser uplink MIMO communications. The former is a key to enabling self-configuring HRISs [13], alleviating their dependence on external control and thus notably facilitating deployment compared with conventional RISs. The latter highlights how, by sensing a portion of the impinging signal, an HRIS can estimate the composite UTs–HRIS channel and contribute to estimating the HRIS–BS channel (see Figure 3). Such estimation is highly challenging when using a solely reflective RIS since, in this case, only the channel outputs at the BS can be observed [15], and the common practice is to resort to estimating the combined channel effect, i.e., the cascaded channel [12], using pilot RIS reflection patterns.

### AOA Estimation

We consider the estimation of the AOA of an impinging signal in quasi free space. For simplicity, we use a 2D square metasurface with  $N$  hybrid meta-atoms (as in the “HRIS Design and Proof of Concept” section) operating at

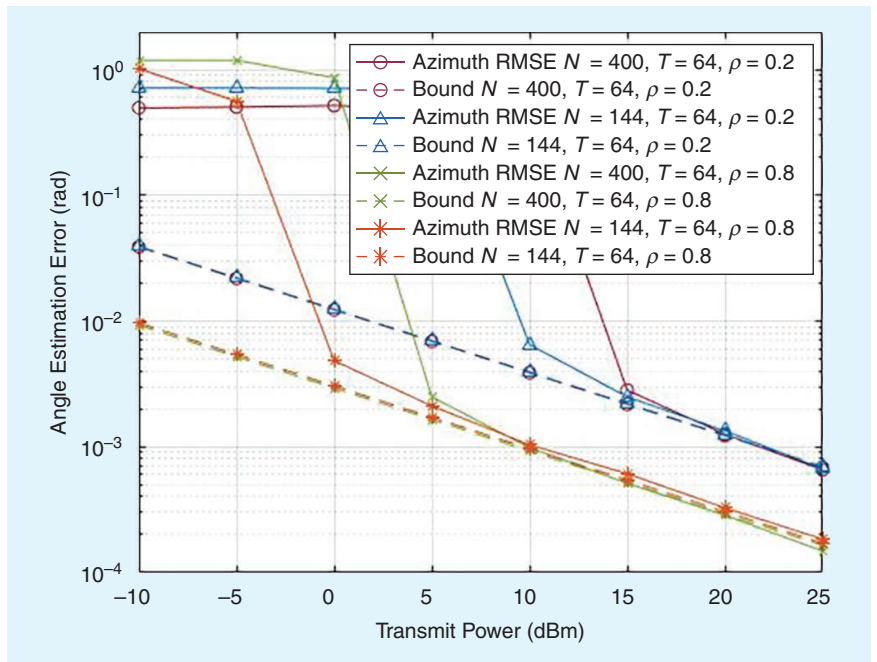


**FIGURE 4** The elevation AOA estimation performance of an HRIS with  $N \in \{144, 400\}$  meta-atoms configured with coupling coefficients  $\rho_n = \rho \in \{0.2, 0.8\}$ ,  $\forall n = 1, 2, \dots, N$ , using  $T = 64$  sensed samples (measurements). The Cramér–Rao lower bounds of the estimations are also included.

19 GHz (corresponding to wavelength  $\lambda = 15.7$  mm) with element spacing of 4 mm ( $\approx \lambda/4$ ) apart. The design frequency is similar to that used in [11] and is considered for demonstration purposes. All meta-atoms are coupled to a single waveguide with the common coupling coefficient  $\rho$ , which is connected to a single reception RF chain. Directive analog combining is used to feed this chain's input, while its digital outputs after  $T$  received samples are used to estimate the AOA by using a maximum-likelihood estimator. While the AOA includes the azimuth and elevation angle, we focus here on the elevation AOA.

The numerically evaluated AOA performance in terms of the root mean square error (RMSE), compared with the Cramér–Rao estimation lower bound, is provided in Figure 4 for  $N \in \{12^2, 20^2\}$ ,  $\rho_n = \rho \in \{0.2, 0.8\}$ ,  $\forall n = 1, 2, \dots, N$ , and  $T = 64$ . As depicted, the AOA of the impinging signal can be accurately estimated even when the portion of the signal being sensed is merely 20% of that incoming. However, as expected, by increasing the meta-atoms' coupling to the waveguide, i.e., by sensing a more dominant portion of the impinging signal, the estimation performance improves. It is also demonstrated that a smaller HRIS yields better performance, which is attributed to the fact that wider beams facilitate AOA estimation. These results demonstrate the ability of HRISs to reliably identify the AOA of an impinging signal, even when only a small portion of it is being sensed while the remainder is reflected.

### Full Channel Estimation

To demonstrate the HRIS channel estimation capability, we consider the uplink system of Figure 3 with  $K$  single-antenna UTs and an HRIS with  $N$  hybrid meta-atoms. The metasurface has  $N_r$  reception RF chains and maintains an out-of-band unidirectional control link with the BS. A simple strategy to estimate the individual channels is to assign the HRIS to estimate the UTs–RIS channel via its sensed observations and to forward this estimate to the BS over the control link (wired or wireless) [5] while changing the phase configuration between pilot symbols, as in [12]. This strategy has similar latency with typical channel estimation schemes for conventional RISs [4]. The fact that the HRIS also reflects while sensing allows the BS to estimate the HRIS–BS channel from its observed reflections, effectively reusing the transmitted pilots for estimating both hops' channels. According to the latter strategy, the HRIS estimates the  $NK$  coefficients comprising the UTs–RIS channel; the measurements are obtained via the  $N_r$  digital signal paths. In the absence of noise, the HRIS is able to recover the UTs–HRIS channel from  $NK/N_r$  pilots, while the BS requires at least  $N$  pilots to recover the HRIS–BS channel, fuzzing its observations and the estimate provided by the HRIS via the control link. For instance, when  $K = 8$  UTs communicate via an HRIS including  $N = 64$  meta-atoms, all attached to  $N_r = 8$  RF chains, both individual channels can be recovered from merely 64 pilots. State-of-the-art methods for conventional RISs would require over 90 pilot transmissions

for recovering solely the cascaded channel for a fully digital 16-antenna BS [12]. However, one needs to also account for the fact that the power splitting between the reflected and sensed waveforms, carried out by the HRIS, affects the resulting SNRs at both the metasurface and BS.

The previously described tradeoff between the MSE performance when estimating the UTs–HRIS channel at the HRIS and the HRIS–BS channel at the BS for different values of the common power splitting parameter  $\rho$  is depicted in Figure 4. The simulation setup consists of a BS with 16 antennas serving eight UTs, assisted by an HRIS with 64 elements and eight RF chains. The UTs are uniformly distributed in a cell with a 10-m radius, where the HRIS is located at the top edge of the cell, and at a distance of 50 m from the BS. The UTs transmit 70 pilot symbols for

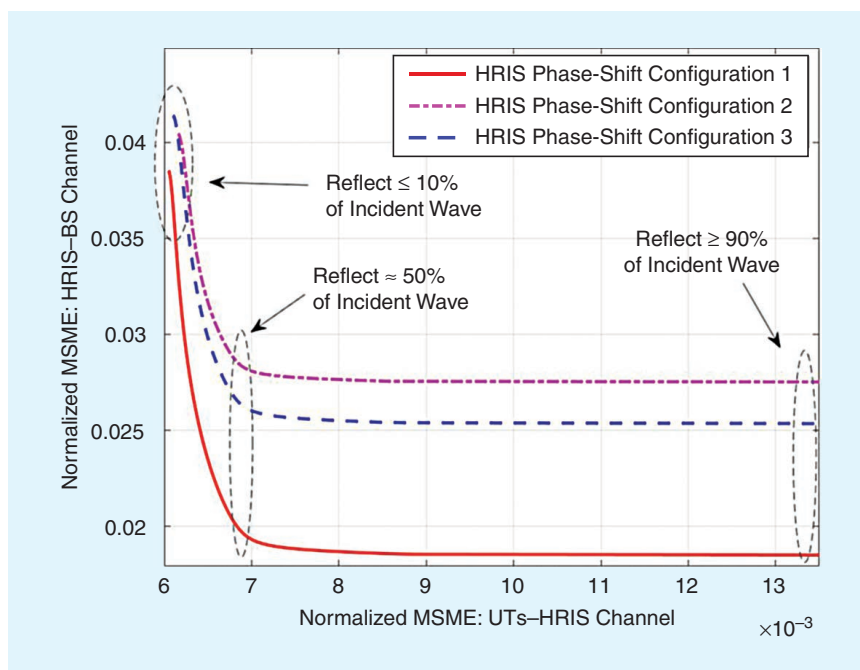


**FIGURE 5** The normalized MSE performance in recovering the composite UTs–HRIS channel at the HRIS and the HRIS–BS channel at the BS, considering a 30-dB transmit SNR as well as different power splitting values  $\rho$  ( $\rho_n = \rho$ ,  $\forall n = 1, 2, \dots, 64$ ) and phase configurations. The fully digital BS is equipped with 16 antenna elements, there exist eight UTs in the system, and the HRIS possesses eight reception RF chains.

channel estimation, which are received at the BS after being reflected by the HRIS, with an SNR of 30 dB. It is observed in Figure 4 that there is a clear tradeoff between the accuracy in estimating each of the individual channels, which is dictated by how the HRIS splits the power of the impinging signal. While the MSE values depend on the HRIS phase configuration, we observe that increasing the portion of the signal that is reflected in the range of up to 50% notably improves the ability to estimate the HRIS–BS channel while having only a minor effect on the MSE of the UTs–HRIS channel estimation. However, further increasing the amount of power reflected notably degrades the MSE in estimating the UTs–HRIS channel while hardly improving the accuracy of the HRIS–BS channel estimation.

The MSE performance in estimating the cascaded channel for the setup in Figure 5 with an HRIS, in comparison to the method in [12] for conventional RISs, is demonstrated in Figure 6. Two different HRIS configurations were considered: a fixed setting, where the coupling parameters  $\forall_n$  were tuned to reflect on average 50% of the incoming signal, and a setting where these parameters were optimized using first-order optimization of the MSE objective by employing automatic differentiation tools [14]. As observed, the sensing capability of HRISs translates into improved cascaded channel estimation, which is more prominent when the parameters  $\forall_n$  are optimized, depending on how many RF chains the HRIS possesses. This behavior stems from the fact that the channel estimation procedure adopted here is geared toward estimating the individual channels without imposing any structure on them and enables the HRIS to estimate the UTs–HRIS locally. While, when the number of RF chains is small, the error induced in such local estimation reflects on the cascaded channel recovery, when employing five RF chains or more, notable performance improvements are observed, though at the cost of higher power consumption and hardware complexity.

### Research Challenges and Opportunities

The design of HRISs and their representative applications provide an indication of the concept’s feasibility and gains. The ability of HRISs to carry out reflection and sensing simultaneously gives rise to a multitude of research challenges and opportunities, as described in the following.

### Fundamental Limits

The inclusion of RF sensing capabilities at metasurfaces considerably changes the operation of metasurface-assisted wireless communication systems. This motivates the characterization of the fundamental limits of HRIS-empowered sensing-aided communications in terms of the achievable rate. Such an analysis can quantify the added value of HRISs compared to solely reflective RISs in a manner that is invariant of the operation of the network end entities.

### Operation Protocols

HRISs provide additional network design degrees of freedom compared to conventional RISs and inherently facilitate integrated sensing and communications schemes, motivating novel algorithmic designs for their exploitation. Their RF sensing, and the relevant computing capabilities, enable signal processing at the metasurface side (e.g., localization and RF mapping), which can be used locally to enable their self-configuration, thus significantly reducing the network overhead for HRIS optimization, or shared to the network for management purposes. In the latter case, efficient low-latency control protocols are needed (possibly among multiple HRISs and BSs) while considering rate-limited in- or out-of-band control links.

### HRIS Modeling

The performance evaluation detailed in the “HRISs for Smart Wireless Environments” section is based on the

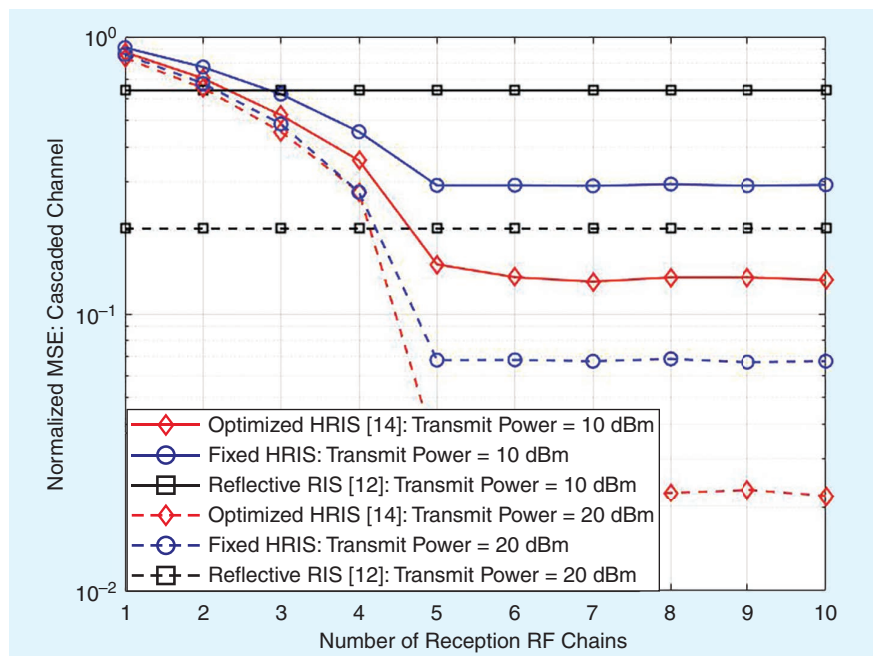


**FIGURE 6** The normalized MSE performance of the cascaded channel estimation as a function of the number of reception RF chains at the HRIS, considering fixed and optimized  $\forall_n$  (via the approach in [14]) for two different transmit power values in dBm. The noise power was set to  $-84$  dBm. The respective estimation performance using a solely reflective RIS, via the scheme of [12], is also included.



presented simplified model for HRIS dual operation. In practice, the EM response of each hybrid meta-atom is expected to exhibit a more complex configurable profile, including coupling between its parameters (i.e., coupling and phase-shifting coefficients) as well as between different elements. Such a physics-driven characterization will allow more faithfully evaluating HRISs. An additional critical aspect that should be characterized is the HRIS excessive power consumption and cost compared to reflective RISs. While such an analysis is expected to be highly implementation dependent, it will help with understanding the price associated with the HRIS gains.

### Hardware Designs

The presented proof of concept, which is based on [9], is an important first step in demonstrating HRIS hardware. Nonetheless, realizing such metasurfaces for wireless operations still requires a large body of experimental efforts and hardware designs, from low up to terahertz frequencies. Akin to purely reflective RISs, the HRIS design requires investigations into the number and pattern of meta-atoms to be implemented as hybrid and their tuning mechanism as well as the overall size of the metasurface and its phase configuration capabilities (e.g., the beam steering span, grating lobes, and sidelobes). All other studies related to forming desired reflection patterns (as done for conventional RISs) are also relevant to HRISs.

### Conclusion

In this article, we reviewed the emerging concept of HRISs for smart wireless environment applications. In contrast to solely reflective RISs, HRISs can simultaneously reflect a portion of the impinging signal in a controllable manner while sensing the other portion of it. We presented an HRIS design and discussed a full-wave EM proof of concept, showcasing the concept's hardware feasibility. We highlighted the possible operations of HRIS-empowered wireless communication systems, provided a simplified model for HRIS reconfigurability, and evaluated the HRIS capability to locally identify AOAs and to facilitate channel estimation in comparison with solely reflective RISs. We discussed several research challenges and compelling new opportunities arising from the HRIS concept, which are expected to pave the way in unveiling the potential of this technology for 6G wireless systems.

### Acknowledgment

The work has been supported by the European Union (EU) Horizon 2020 Reconfigurable Intelligent Sustainable Environments for 6G (RISE-6G) Wireless Networks project, under Grant 101017011, and the Smart Networks and Services Joint Undertaking project Terahertz Reconfigurable Metasurfaces (TERRAMETA) for Ultra-High Rate Wireless Communications, under the EU's Horizon Europe research and innovation program, under Grant

101097101, including top-up funding by UK Research and Innovation, under the United Kingdom's Horizon Europe funding guarantee.

### Author Information



**George C. Alexandropoulos** (alexandg@di.uoa.gr) is an associate professor in the Department of Informatics and Telecommunications, National and Kapodistrian University of Athens, 15784 Athens, Greece. His research interests include algorithmic design and performance analysis for wireless networks, with emphasis on multiantenna transceiver hardware architectures, active and passive metasurfaces, full-duplex radios, and millimeter-wave/terahertz communications, as well as distributed machine learning algorithms. He is a Senior Member of IEEE.



**Nir Shlezinger** (nirshl@bgu.ac.il) is an assistant professor in the School of Electrical and Computer Engineering, Ben-Gurion University of the Negev, Beer-Sheva 85105, Israel. He is a Senior Member of IEEE.



**Idban Alamzadeh** (idbanaz@asu.edu) is working toward the Ph.D. degree in electrical engineering at Arizona State University, Tempe, AZ 85281 USA.



**Mohammadreza F. Imani** (mohammadreza.imani@asu.edu) is an assistant professor in the School of Electrical, Computer, and Energy Engineering, Arizona State University, Tempe, AZ 85281, USA. He is a Member of IEEE.



**Haiyang Zhang** (20220142@njupt.edu.cn) is a professor in the School of Communication and Information Engineering, Nanjing University of Posts and Telecommunications, Nanjing, China. He is a Member of IEEE.



**Yonina C. Eldar** (yonina.eldar@weizmann.ac.il) is a professor in the Department of Mathematics and Computer Science, Weizmann Institute of Science, Rehovot 7610001, Israel. She is a Fellow of IEEE.

### References

- [1] "The next hyper-connected experience for all," Samsung 6G Vision, White Paper, Jun. 2020. [Online]. Available: <https://cdn.codeground.org/nsr/downloads/researchareas/6G%20Vision.pdf>
- [2] C. Huang et al., "Reconfigurable intelligent surfaces for energy efficiency in wireless communication," *IEEE Trans. Wireless Commun.*, vol. 18, no. 8, pp. 4157–4170, Aug. 2019, doi: 10.1109/TWC.2019.2922609.
- [3] Q. Wu et al., "Intelligent reflecting surface-aided wireless communications: A tutorial," *IEEE Trans. Commun.*, vol. 69, no. 5, pp. 3313–3351, May 2021, doi: 10.1109/TCOMM.2021.3051897.

- [4] M. Jian et al., "Reconfigurable intelligent surfaces for wireless communications: Overview of hardware designs, channel models, and estimation techniques," *Intell. Converged Netw.*, vol. 3, no. 1, pp. 1–32, Mar. 2022, doi: 10.23919/ICN.2022.0005.
- [5] E. Calvanese Strinati et al., "Reconfigurable, intelligent, and sustainable wireless environments for 6G smart connectivity," *IEEE Commun. Mag.*, vol. 59, no. 10, pp. 99–105, Oct. 2021, doi: 10.1109/MCOM.001.2100070.
- [6] K. Keykhosravi et al., "Leveraging RIS-enabled smart signal propagation for solving infeasible localization problems: Scenarios, key research directions, and open challenges," *IEEE Veh. Technol. Mag.*, vol. 18, no. 2, pp. 20–28, Jun. 2023, doi: 10.1109/MVT.2023.3237004.
- [7] A. Taha et al., "Enabling large intelligent surfaces with compressive sensing and deep learning," *IEEE Access*, vol. 9, pp. 44,304–44,321, 2021, doi: 10.1109/ACCESS.2021.3064073.
- [8] N. Shlezinger et al., "Dynamic metasurface antennas for 6G extreme massive MIMO communications," *IEEE Wireless Commun.*, vol. 28, no. 2, pp. 106–113, Apr. 2021, doi: 10.1109/MWC.001.2000267.
- [9] I. Alamzadeh et al., "A reconfigurable intelligent surface with integrated sensing capability," *Sci. Rep.*, vol. 11, no. 1, pp. 1–10, 2021, doi: 10.1038/s41598-021-99722-x.
- [10] C. Liaskos et al., "ABSense: Sensing electromagnetic waves on metasurfaces via ambient compilation of full absorption," in *Proc. 6th Annu. ACM Int. Conf. Nanoscale Comput. Commun. (NANOCOM)*, Dublin, Ireland, Sep. 2019, pp. 1–6.
- [11] T. Sleasman et al., "Microwave imaging using a disordered cavity with a dynamically tunable impedance surface," *Phys. Rev. Appl.*, vol. 6, no. 5, 2016, Art. no. 054019, doi: 10.1103/PhysRevApplied.6.054019.
- [12] Z. Wang et al., "Channel estimation for intelligent reflecting surface assisted multiuser communications: Framework, algorithms, and analysis," *IEEE Trans. Wireless Commun.*, vol. 19, no. 10, pp. 6607–6620, Oct. 2020, doi: 10.1109/TWC.2020.3004330.
- [13] A. L. Moustakas et al., "Reconfigurable intelligent surfaces and capacity optimization: A large system analysis," *IEEE Trans. Wireless Commun.*, early access, 2023, doi: 10.1109/TWC.2023.3265420.
- [14] H. Zhang et al., "Channel estimation with hybrid reconfigurable intelligent metasurfaces," *IEEE Trans. Commun.*, vol. 71, no. 4, pp. 2441–2456, Apr. 2023, doi: 10.1109/TCOMM.2023.3244213.
- [15] C. Hu et al., "Two-timescale channel estimation for reconfigurable intelligent surface aided wireless communications," *IEEE Trans. Commun.*, vol. 69, no. 11, pp. 7736–7747, Nov. 2021, doi: 10.1109/TCOMM.2021.3072729.

VT